Tellus A
Dynamic Meteorology and Oceanography

Contributions from Changing Large-Scale Atmospheric Conditions to Changes in Scandinavian Temperature and Precipitation Between Two Climate Normals

ORIGINAL RESEARCH PAPER

ERIK KJELLSTRÖM
FELICITAS HANSEN
DANIJEL BELUŠIĆ
Author affiliations can be found in the back matter of this article

STOCKHOLM UNIVERSITY PRESS

ABSTRACT

Multidecadal changes in regional climate can occur as a forced response to changing greenhouse gases and aerosols, as a result of natural internal climate variability, or due to their combination. Internal climate variability is frequently associated with regional changes in large-scale circulation. We investigate how changes in Scandinavian temperature and precipitation conditions during 1961–2020 can be linked to changes in the atmospheric large-scale circulation. The study is based on data from the ERA5 reanalysis and on Swedish average conditions based on observations from the Swedish Meteorological and Hydrological Institute. In general, it is shown that all seasons have become warmer and there is a predominance for more precipitation in the last 30 years. The results also show a clear decrease in daily temperature variability for winter and an increase in summer while there is no similar systematic change for precipitation. Further, we use a circulation type classification technique for identifying ten different circulation types for each calendar month in the 1961–2020 period. Results indicate that changes between the two periods can partly be related to changes in large-scale circulation due to changes in the frequencies of different circulation types. However, it is also clear that the contribution from frequency-related changes to the total change is comparatively low for most months and that changes also within the circulation types are required to explain the total change. The main conclusion of the study is that during the last 30 years it has mostly been warmer than in the preceding 30 years for the same type of weather situation for all months in the year. Consequently, internal climate variability, as represented by changes in the large-scale atmospheric circulation, cannot explain the observed changes in the Scandinavian temperature and precipitation.

CORRESPONDING AUTHOR:
Erik Kjellström
Rossby Centre, Swedish Meteorological and Hydrological Institute, SMHI, Norrköping, SE-602 19, SE; Department of Meteorology and Bolin Centre for climate research, Stockholm University, Stockholm, SE-106 91, SE
erik.kjellstrom@smhi.se

KEYWORDS:
weather type classification; circulation type; climate change; reanalysis; Sweden

TO CITE THIS ARTICLE:
Kjellström, E., & Hansen, F., & Belušić, D. 2022. Contributions from Changing Large-Scale Atmospheric Conditions to Changes in Scandinavian Temperature and Precipitation Between Two Climate Normals. *Tellus A: Dynamic Meteorology and Oceanography*, 74(2022), 204–221. DOI: *https://doi.org/10.16993/tellusa.49*

INTRODUCTION

Ongoing global warming, resulting primarily from increasing greenhouse gas concentrations in the atmosphere (IPCC, 2021), is rapid and comes with strong global and regional impacts (IPCC, 2018). In a European perspective warming is pronounced both in winter and summer. The Arctic region shows particularly strong temperature increase, resulting from feedback mechanisms involving retreating snow and ice cover (IPCC, 2019). At the same time, the North Atlantic does not warm as rapidly; and one of the areas where the lower atmosphere warming is smallest on a global scale is found south of Greenland (Gulev et al., 2021). In summer, the Mediterranean area is subject to strong warming. Many of these features are seen in observations and are expected to become even more pronounced in the future as a consequence of continued global warming. Resulting from such geographical differences and depending on the large-scale circulation of the atmosphere, other nearby areas, including northern Europe, may see variational changes with time in climate characteristics such as near surface temperature and precipitation. Such changes represent different signatures of climate change and involve changes both in seasonal means as well as changes in higher order statistics such as daily variability (Kjellström, 2004).

Changes in the large-scale atmospheric circulation and variability on longer time scales from years to decades contribute significantly to uncertainty in projections of future climate change for the 21st century (van Ulden and van Oldenborgh, 2006; Kjellström et al., 2011). The contribution has been shown to be especially important to the overall climate uncertainty in small regions and for the near future when anthropogenic climate forcing is still relatively small (Hawkins and Sutton, 2009). Change and variability in large-scale circulation is strongly related to the frequency of different circulation patterns. For instance, periods can have more or less zonal or meridional winds, which have strong consequences for weather and climate conditions including extremes such as cold winters (Cattiaux et al., 2010) and warm summers (Wilcke et al., 2020). Specifically, for Europe, such episodes can to a strong degree be linked to the North Atlantic Oscillation (NAO), which in its positive phase is indicative of zonal flow and advection of maritime influenced air masses from the North Atlantic (Hurrell, 1995). Trends in the large-scale circulation, such as manifested by changes in the NAO index, can potentially have strong impacts on the regional climate, as shown by e.g. Hegerl et al. (2018). There are also changes in the large-scale circulation that may be related to long-term forcing-derived trends, such as greenhouse gas concentrations or aerosols, or natural variability in for example sea surface temperatures or soil moisture. As an example, Cattiaux et al. (2010) showed that the cold European winter 2010 was warmer than expected from its record-breaking seasonal circulation pattern. They concluded that this provided a picture of a regional cold event mitigated by long-term climate warming.

The large variability from year to year or decade to decade implies that climate change can be difficult to detect as changes on local and regional scales may reflect erratic changes in the large-scale circulation (Rutgersson et al., 2014). An implication is that different long-term climate change features associated with global warming, such as regional warming or changing precipitation, emerge at different times due to different degrees of variability (Hawkins and Sutton, 2012). For example, Kjellström et al. (2013) showed that changes in seasonal mean temperatures in Europe are readily discernible out of the background noise, related to large interannual and decadal variability, already in the first decades of the 21st century, while corresponding discernible changes in precipitation lags by several decades or more. Strong natural variability in the large-scale circulation may also impede attribution of regional climate change to the ongoing anthropogenically forced global warming (Hegerl and Zwiers, 2011). Despite this a number of attribution studies for the European and North Atlantic region have been conducted. For Northern Europe Bhend and von Storch (2009) found that the increase in annual mean temperatures in the Baltic Sea region could be linked to the ongoing global warming but that it was not possible to make such statements for changes in individual seasons or for spatial patterns. More recently, Parding et al. (2016) found that changes in the large-scale circulation contributed to explaining the warming in Northern Europe in addition to the increased greenhouse gas content but that also other effects, such as decreasing aerosol emissions, were needed to fully account for the observed changes. Attribution studies have also focused on earlier time periods; for instance, Hegerl et al. (2018) found that changes in the first half of the 20th century resulted from a combination of changes in large-scale circulation, greenhouse gas concentrations and aerosol content of the atmosphere.

One way of describing and understanding impacts of variations in the large-scale atmospheric circulation is through analysis of weather types or circulation types (CTs). A large number of methods to assemble meteorological data into distinct CTs have been used for this purpose (see Philipp et al., 2010 for a review). Busuioc et al. (2001) found a strong dependence on precipitation in Sweden between 1890 and 1990 on the large-scale circulation based on an EOF analysis. In addition to classifying large-scale patterns into CTs, Barry and Perry (1973) decomposed climate differences into different parts that are caused either by changes in frequency or changes within each CT. This methodology has subsequently been widely applied. For instance, Beck et al. (2007) found that large parts of the long-term variations at a number of stations in the Central European climate since 1780

cannot be explained just by frequency changes of CTs. Similarly, but involving spatial fields covering all of Europe, Kuettel et al. (2011) found that wintertime changes over the last 250 years are strongly related also to within-CT changes, in particular for temperature in Eastern Europe and Scandinavia. For more recent decades, Cahynova and Huth (2016) showed a significant trend for changes in the frequency of CTs in 1961–2000 that could explain part of the changes in temperature and precipitation in Europe. Such methods have also been used for extremes, including Sui et al. (2020) showing that within-CT changes were mostly responsible for the positive trend in warm extremes and the negative trend in cold extremes for wintertime conditions in Northern Europe from 1979 to 2016. One of the circulation type classification (CTC) methods extensively used is the simulated annealing and diversified randomization (SANDRA) classification scheme (Philipp et al., 2007). It has been shown to perform comparatively well (Philipp et al., 2016) and by adding a step of a simple pre-processing of input data Hansen and Belušić (2021) recently showed that the SANDRA method results in even more physically consistent CTs compared to previous studies.

The motivation for this work is to extend previous analysis of impacts from large-scale circulation changes to the full period 1961–2020 looking at changes in temperature and precipitation in Northernmost Europe for all seasons. By applying the SANDRA CTC method, as adopted by Hansen and Belušić (2021), we investigate how Scandinavian/Swedish temperature and precipitation conditions can be linked to the large-scale atmospheric circulation. Specifically, we ask the question to what degree changes in large-scale circulation can explain the observed changes in temperature and precipitation. Here, we apply the Barry and Perry (1973) decomposition on reanalysis fields to distinguish between changes related to CT frequency or to alterations within CTs. We focus on monthly mean conditions for which the CTC is performed but also investigate changes in daily variability. A further motivation for the study has been a wish for better categorizing differences between the two climate normals 1961–1990 and 1991–2020.

DATA AND METHOD

DATA

The main part of the analysis has been done based on reanalysis data from ERA5 from the European Centre for Medium range Weather Forecasts (Hersbach et al., 2020). We have used daily mean sea level pressure, near-surface temperature and precipitation. The analysis has been made based on data from January 1st 1961 to November 26th 2020. For comparison of results with the NAO we have used data for monthly NAO-index values provided by NCAR (2021). They have derived the index based on an EOF analysis according to Hurrell (2003).

To set the analysis in a Swedish context we have used i) data from ERA5 and ii) two climate indicators from the Swedish Meteorological and Hydrological Institute (SMHI). The two indicators are areal averages for Sweden of near-surface temperature and precipitation. For temperature this is based on data from 35 stations spread out over the country while for precipitation the number of stations is approximately 80. Results for Sweden are also compared to the northern hemisphere average from HadCRUT5 (Morice et al., 2021).

CIRCULATION TYPE CLASSIFICATION TECHNIQUE

For the determination of CTs and the assignment of individual days to them, the simulated annealing and diversified randomization (SANDRA) clustering scheme (Philipp et al., 2007) is used. SANDRA is a non-hierarchical clustering technique based on conventional k-means clustering which attempts to minimize the sum of Euclidean distances within a class while at the same time maximizing the distances between different classes. In the process of simulated annealing, the overall data partitioning quality is allowed to be temporarily decreased, but the resulting set of CTs is closer to the "global optimum" than, e.g., in standard k-means clustering. In addition to overcoming many of the limitations of other automated clustering methods, SANDRA is at the same time also less numerically expensive.

The SANDRA method is used with daily mean SLP fields with the spatial mean removed. Hansen and Belušić (2021) showed recently that this simple pre-processing of input data results in both physically more consistent CTs compared to when unprocessed data is used and a better partitioning of independent variables like temperature or precipitation. Ten CTs are calculated based on the full time series 1961–2020 for each month separately.

DISCRIMINATION INTO FREQUENCY AND INTENSITY

The climate change signal between 1961–1990 and 1991–2020 has been divided in two parts following Barry and Perry (1973). One part is related to changes in frequency of the respective CTs while the other part deals with changes within the respective CTs. Formally, the total change is given by

$$\Delta C = \sum_{i=1}^{G} \left[\Delta F_i \left(C_i + \Delta C_i \right) / n + F_i \Delta C_i / n \right] \qquad (1)$$

where

G = the number of CTs (here 10)
F_i = the frequency of CT i during the first period
$F_i + \Delta F_i$ = the frequency of CT i during the second period
n = number of time steps during the first period
C_i = climatological average for CT i during the first period
$C_i + \Delta C_i$ = climatological average for CT i during the second period

RESULTS

TEMPERATURE AND PRECIPITATION IN SWEDEN OVER THE LAST SIXTY YEARS

The Scandinavian area has seen strong climate change over the last 60 years. ***Figure 1*** shows how the annual mean temperature and precipitation has changed between the two climate normals 1961–1990 and 1991–2020 according to ERA5. Changes are largest in mountainous regions in Norway and Sweden but warming is also pronounced over parts of the Baltic Sea and Finland. Correspondingly, precipitation has increased in large parts of the area, again with the largest changes in connection to mountainous areas in Norway and Sweden. We can also note an increase in precipitation in western parts of southern Sweden and more generally in northern Sweden and Finland. In the southeast, precipitation has instead decreased.

For Sweden as an average, SMHIs long-term temperature record and ERA5 both show c. 1.1°C higher annual mean temperatures in the latter period which may be compared to the Northern Hemisphere average change of 0.72°C as given by HadCRUT5. For precipitation, the Swedish average given by the ERA5 shows an increase of 3.4% while the average compiled from the climate stations indicates an increase of 6.7% on an annual mean basis. Corresponding station-based numbers for Swedish mean temperature and precipitation changes for the three-month nominal seasons are given in ***Table 1***. It is clear that all seasons have become warmer in the second period. The inter-annual variability, expressed as one standard deviation around the mean, has decreased for winter and increased for summer and fall. For precipitation the latter period shows more precipitation for all seasons although differences are relatively small

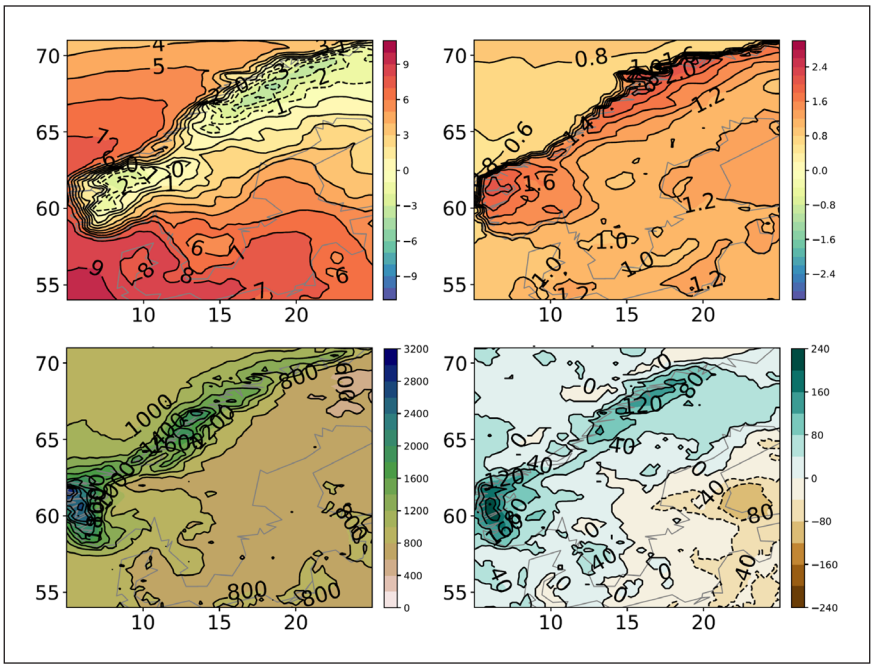

Figure 1 Annual mean temperature (°C; 1st row) and precipitation (mm; 2nd row) in the Scandinavian area for 1961–1990 (left) and changes between 1991–2020 and 1961–1990 (right). Data are taken from the reanalysis ERA5.

NORMAL PERIOD	SEASON	TEMPERATURE		PRECIPITATION	
		MEAN ± 1 Σ	MIN/MAX	MEAN ± CV	MIN/MAX
1961–1990	DJF	−4.6 ± 2.6	−9.5 / −0.5	133 ± 26	72 / 203
	MAM	3.2 ± 1.1	1.4 / 5.9	115 ± 26	49 / 158
	JJA	14.6 ± 0.8	12.7 / 16.1	203 ± 20	122 / 285
	SON	5.6 ± 0.9	3.5 / 7.9	193 ± 17	129 / 267
1991–2020	DJF	−2.8 ± 2.0	−6.9 / 0.9	148 ± 23	47 / 195
	MAM	4.4 ± 1.0	2.5 / 5.9	120 ± 20	84 / 174
	JJA	15.4 ± 1.0	13.3 / 17.3	229 ± 17	153 / 309
	SON	6.3 ± 1.2	3.9 / 8.2	188 ± 18	139 / 269

Table 1 Mean temperature (°C) and precipitation (mm) in Sweden from SMHIs climate indicators. Interannual variability is given as one standard deviation for temperature and as the standard deviation normalised with the mean for precipitation to give the coefficient of variation (CV that is given in %).

for spring and fall. In this case there is a tendency for reduced variability in all seasons apart from fall.

CIRCULATION TYPE BASED 60-YEAR CLIMATOLOGY

The CTC analysis based on the full period 1961–2020 results in distinct patterns of mean sea level pressure and associated near surface temperature and precipitation for the Scandinavian area as shown in the composite plots for January and July in ***Figures 2*** and ***3***. The CTs are shown in order of frequency where CT1 (Circulation Type number 1) is the most frequent cluster for each month which implies that CTs with the same number in ***Figures 2*** and ***3*** are not necessarily describing the same atmospheric circulation pattern. Despite differences in frequency between CTs in individual months the analysis shows that the large-scale circulation patterns are similar throughout the year (not shown). Similarities are notably strong among the winter months and among the summer months with a gradual transition in between during fall and spring.

For January (***Figure 2***), the most common CT (CT1) shows a high-pressure ridge over Finland and Scandinavia with associated weak winds from the east or northeast over southern Sweden and winds from the south or southwest over the mountain ridge and in the far north. The situation is associated with cold conditions over most of the country while precipitation is below, albeit close to, its average. Seen as an average over the whole country, CT1 is the coldest second only to CT9 that has a similar large-scale circulation although with stronger easterlies reaching further to the north. Both clusters show relatively dry conditions but in CT9 there is more precipitation in the south in association with the low-pressure system to the southeast of the Baltic Sea. Contrastingly, CT3, CT4 and CT7 show warmer than average conditions and winds from the west or southwest over most of the area. These CTs are also associated with high precipitation, in particular along the west coast of Norway due to the orographic reinforcement. Also, CT10 shows strong westerlies in the southern half of the domain while the northeasternmost part is dominated by weak anticyclonic conditions. For CT5 there is also a clear difference between a strong south-westerly flow in the north with mild and above average precipitation and a high-pressure situation in the south dominated by colder conditions and less precipitation than average. CT2 is associated with a more northerly flow and thereby relatively cold and dry conditions while CT6 and CT8 represent situations with winds from the south indicative of warmer conditions and more precipitation than average. For CT6 this is, however, modified in the far north where winds are more easterly leading to relatively cold conditions.

For summer the CTs represent distinctly different pressure patterns as shown for July in ***Figure 3***. In general, pressure is higher and pressure gradients weaker, indicative of weaker winds, than in winter. The most high-pressure dominated situations are CT1 and

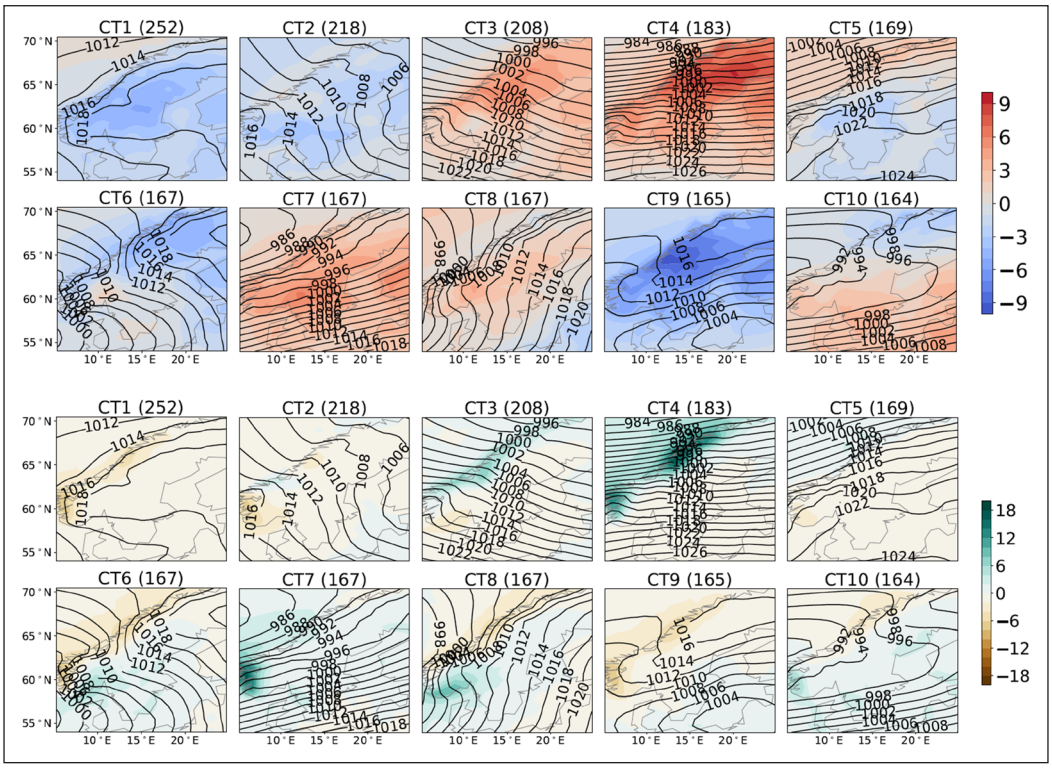

Figure 2 Ten circulation types generated using the SANDRA CTC method for all January days in 1961–2020. The frequency for each cluster is indicated as the number of days (out of a total of 1860) on top of each map. The isolines show composite averages mean sea level pressure. The colour shaded fields show corresponding temperature and precipitation anomalies relative to the monthly mean for temperature (top, °C) and precipitation (bottom, mm).

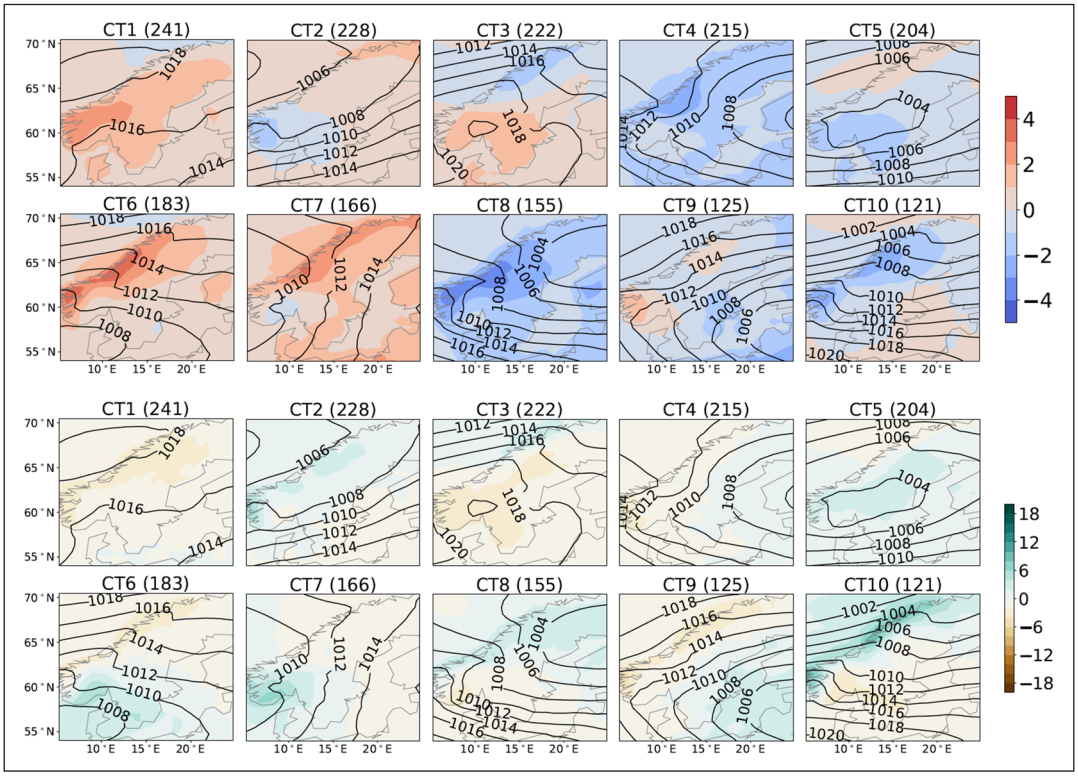

Figure 3 As Figure 2, except for July.

CT3 with temperatures above average in all of Sweden apart from the northernmost part of the mountain chain in CT3 where low pressures north of Scandinavia brings relatively cold and wet conditions. Apart from that, precipitation is below average in both CTs. CT5 is dominated by a low-pressure pattern with cold and wet conditions apart from the far north that has relatively mild conditions. Low pressure dominates in the north in CT8 with above average precipitation and cold conditions. Furthermore, cold air masses are being advected from the north bringing cold conditions also to southern parts of Scandinavia. CT2 and CT10 are both indicative of low-pressure conditions over the North Atlantic that yield winds around west to southwest over large parts of Sweden with colder and wetter than average conditions. In some more detail it is clear that CT2 shows different precipitation amounts between western and southern parts of southern Sweden as a consequence of orographic reinforcement. Likewise, in CT10, most precipitation falls in Norway leading to drier than average conditions in Sweden apart from the northern parts of the mountain chain. CT6 and CT7 are associated with low-pressure centres southwest and west of Scandinavia bringing winds around east or southeast over Sweden and relatively warm conditions. Southern Sweden receives more precipitation than average while there is less than average in the north. In CT4 and CT9 the low-pressure centres are more to the east indicating winds around north or northeast over the country. Consequently, conditions in Sweden are generally relatively cold, and in the east with more precipitation than average.

CT BASED CLIMATE CHANGE SIGNAL

In this section we look separately at the two time periods 1961–1990 and 1991–2020. Analysis is done both for frequency of the respective ten CTs for each month as well as for changes within each CT.

Changes in monthly mean conditions

Figure 4 shows how the frequency of the respective CTs change between the two periods for each month. Note that the numbering of the CTs is done for each month separately indicating that the individual months cannot be directly compared to each other. It is clear that the frequencies for the respective CTs are similar between the two periods. For instance, CT1, the most common CT in the 60-year time series, is most common in both individual periods for five months (February, March, April, August and December). Similarly, CT10 is the rarest one in both periods for February, April, May, June and July. Also, in other cases, CTs with high frequency in one period generally show high frequency also in the other period. But there are exceptions to this, like for instance CT9 in January that occurs about twice as often in 1961–1990 as in 1991–2020. For July, we note that CT3 was much more common in 1961–1990 while CT6 was more common in 1991–2020.

For each CT we show the differences between the two periods for January and July in ***Figures 5*** and ***6***. For all CTs we note some differences in surface pressure. Mostly these differences are relatively weak but we can see that the situation for CT9 in January changes markedly between the periods. Here, the high-pressure ridge in the

north is considerably weakened in the second period. At the same time, the low in the southeast is much deeper and shifted towards the north. As a result, the north-south pressure gradient in the region is of about equal strength.

Apart from the changes in surface pressure it is clear that the majority of the CTs reveal warmer conditions in the second period. An exception is CT4 with slightly colder conditions in parts of northern Sweden. In this case we note that the north-south pressure gradient

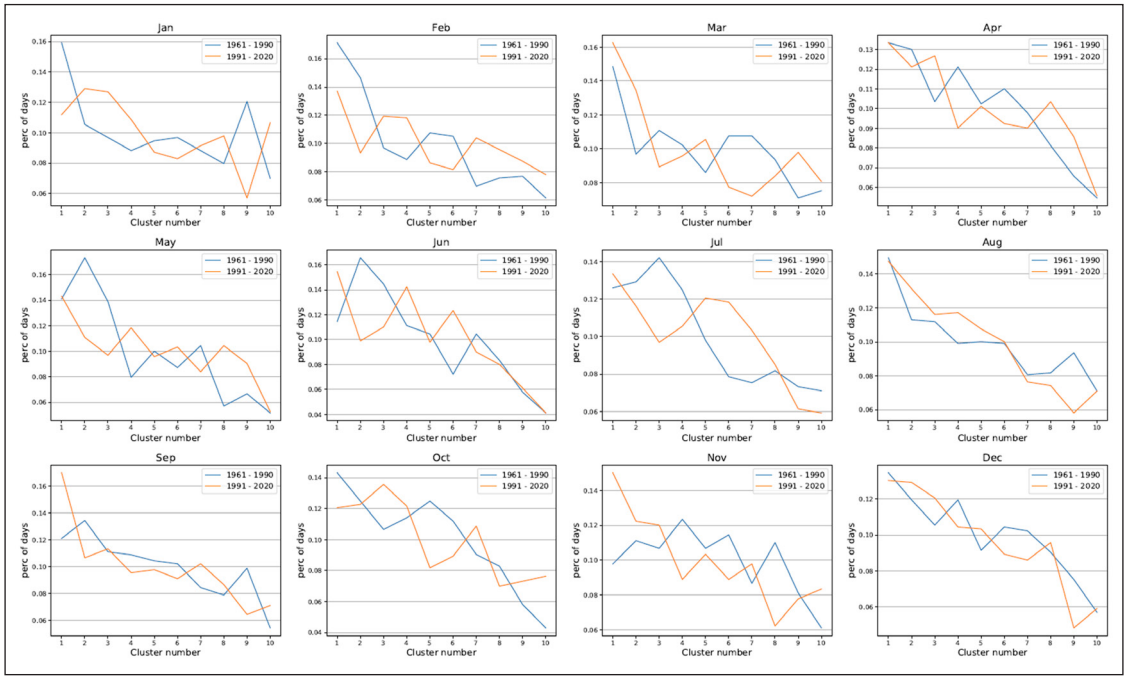

Figure 4 Frequencies for each circulation type in the two periods for 1961–1990 (blue) and 1991–2020 (orange). Note that circulation types are defined separately for each month and that it is not meaningful to compare the individual circulation type numbers between months.

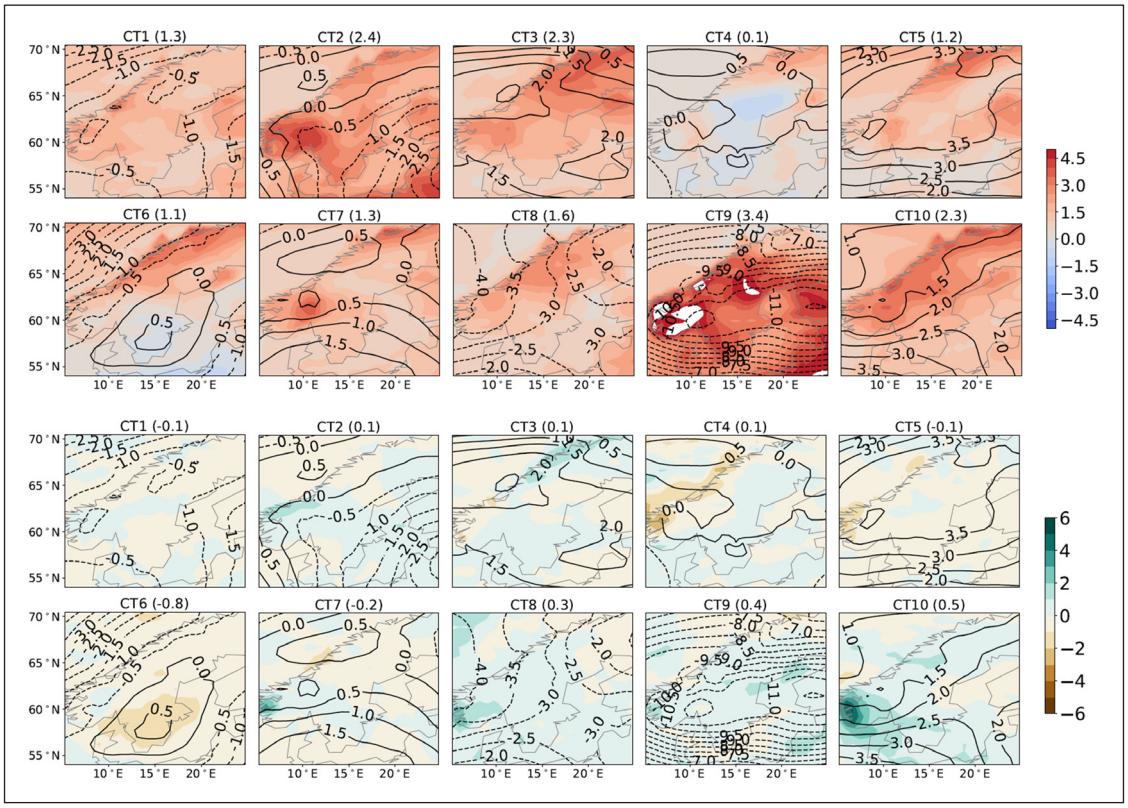

Figure 5 Difference for each circulation type in January (cf. Figure 2) between 1961–1990 and 1991–2020. The isolines show average change in mean sea level pressure. The colour shaded fields show corresponding changes in temperature (top, °C) and precipitation (bottom, mm). The numbers given on top of the panels are the average changes over Sweden between the two periods.

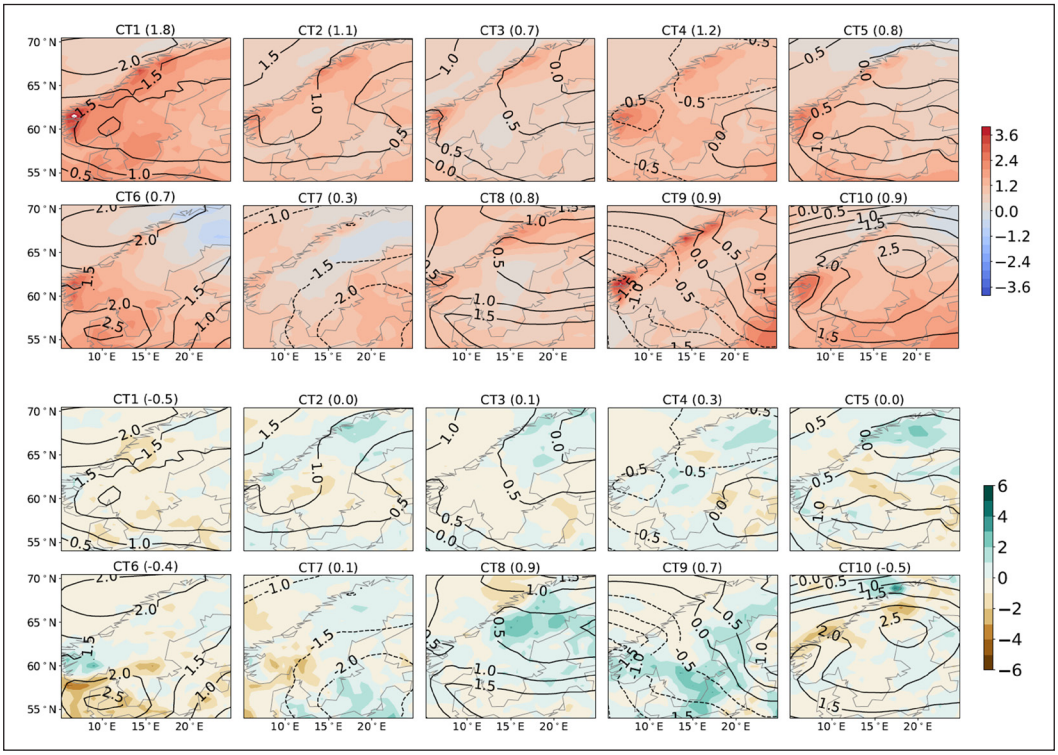

Figure 6 As Figure 5, except for July (cf. Figure 3).

off the Norwegian coast is slightly weaker which contributes to weaker winds towards Scandinavia that, in turn, influences both precipitation and temperature conditions. Also, in CT6 there are areas in the south where a slight reduction in temperatures are seen, likely in connection with a somewhat stronger high-pressure ridge stretching over the country from the north-east. Apart from these two exceptions in CT4 and CT6 we note higher temperatures in all situations in the second period. Differences in precipitation between the two periods show areas with more and areas with less precipitation for all clusters. Differences are, in several cases, particularly strong along the Norwegian west coast, which may be linked to orographic reinforcement. But also changes in temperature, and thereby atmospheric content of water vapor, may play a role as well as changes in pressure gradients. An example of the latter is CT3, where the north-south pressure gradient is strengthened north of c. 65°N with increasing precipitation along the Norwegian coast. South of 65°N where the pressure gradient is weakened, precipitation instead decreases. In Sweden we note, in particular, increased precipitation in CT10 which is associated with low pressure systems moving in from the North Atlantic. In the cold CT9 we also note more precipitation, in particular in the north, indicative of snowfall along the coast. Also in the southerly dominated CT8 precipitation has increased in most of the country. In all these three CTs we note strengthening of the pressure gradients (cf. ***Figure 2***) in parts of the domain indicating stronger transport of water vapor and thereby, more precipitation. In CT10 this involves a sharpening of the north-south pressure gradient south of the low pressure in the west contributing to widespread precipitation increase in the southern part of the domain. In CT9 the north-south pressure gradient over the northern part of the Baltic Sea becomes stronger leading to stronger easterlies and more precipitation in northern Sweden. In CT8, finally, the east-west pressure gradient is increased contributing to more precipitation in the southerly flow over Scandinavia. The only cluster showing considerable decrease of precipitation over Sweden is CT5, which may be related to the somewhat more pronounced high-pressure ridge over the country as described above.

Also for July (***Figure 6***) there is a clear increase in temperature in most CTs with the exceptions of CT6 and CT7 over parts of northernmost Sweden. For CT7 lower pressure in the whole domain with a weaker high pressure in the east and a deeper low pressure in the west reveals a situation more characterized by cyclonic conditions. Also, a slight weakening of the east-west pressure gradient indicates weaker southerlies in the second period that may have contributed to the lower temperatures in the north. For CT6, a slightly stronger pressure gradient in the far north indicates stronger north-easterly winds over northernmost Scandinavia that may more efficiently bring in colder air masses from the north to the area. In the southwest part of the domain this cluster is associated with a strong increase in pressure and associated warmer and drier conditions. For the high-pressure influenced CT1, we note that the pressure increases in the entire domain and mostly so in the north. This CT is associated with strong temperature increases with maxima both along the mountain chain in the north and in the south-eastern parts of Sweden.

Associated with this CT is also a decrease in precipitation, in particular in the north, likely a result of the more anticyclonic conditions. For the other high-pressure dominated cluster, CT3, changes in pressure are relatively small albeit with a tendency for a stronger high-pressure ridge extending further to the east towards the Baltic countries. This is also an area with decreasing precipitation while it increases in the northernmost part. The temperature increases associated with CT3 are smaller than those in CT1. Also the low-pressure dominated CT4 (east part of the domain), CT5, CT8 (northeast) and CT9 (southeast) show increasing temperature. The largest increases in precipitation are associated with the low-pressure systems in the northern parts in CT8 and over parts of southern Scandinavia and along the northern Baltic Sea coast in CT9. For both of these CTs there are changes in the pressure patterns although these are relatively small in the vicinity of the low-pressure centres where most precipitation falls (cf. ***Figure 3***). In both cases the precipitation increases are pronounced in areas with winds from the north or northeast.

Summarizing for Sweden we note that in the majority of CTs for all months 1991–2020 is warmer compared to 1961–1990. It is only in eight out of 120 combinations that a CT is colder in the second period (***Table 2***). We can also compare with the Northern Hemisphere average as given by HadCRUT5, which ranges from 0.65°C in June to 0.80°C in January and note that the warming is stronger in 74 of the 120 cases (***Table 2***). Adding up we find that in 20 of the 120 cases warming within a CT is more than twice that seen in the northern hemisphere average. For January and July as discussed above, the majority of the CTs show larger warming than the northern hemisphere average. In particular in January we note five CTs showing more than twice the Northern Hemisphere warming rate. It is only in CT4 in January when warming is smaller than the hemispheric average, which is not surprising as this CT is dominated by westerly winds bringing air from the North Atlantic that has warmed relatively little.

For Swedish mean precipitation the picture reveals a larger fraction of cases with increased precipitation than cases with decreases (***Table 3***). In total 57 out of 120 combinations show precipitation increase with more than 5% and 16 with more than 25% increase. Corresponding numbers for decreases are 38 and 8 combinations.

Changes in daily variability of temperature and precipitation

Figure 7 shows distributions of daily areal averages for Sweden for each respective CT in the two periods. Again, the warming is clearly seen in the means and medians. But the distributions also indicate differences in the signature of the warming. For some CTs, changes are larger than in others and with different amplitudes for lower ends of the distributions compared to those for the upper ends. Notably, the interquartile range shrinks for most clusters in January. This is primarily a result of a stronger increase in temperature on the cold side of the distribution with the 25th percentile increasing relatively more than the 75th. Exceptions to this general pattern involve the warmest CT4 for which the interquartile range increases, the coldest (CT9) where the interquartile range is roughly unchanged, although centred at much higher temperatures and CT10 that also reveals a mere shift in the distribution. For July the situation is reversed: all CTs, apart from two, show increased interquartile

	1	2	3	4	5	6	7	8	9	10	NH
JAN	*1.3*	*2.4*	*2.3*	**0.1**	*1.2*	*1.1*	*1.3*	*1.6*	3.4	2.3	0.74
FEB	*1.5*	**0.7**	*3.3*	1.1	*0.5*	*0.1*	0.0	*2.8*	*1.9*	*0.7*	0.80
MAR	*1.8*	*1.5*	*0.8*	0.5	*2.1*	0.8	0.7	*0.6*	0.8	*1.5*	0.78
APR	1.3	1.6	**1.2**	*1.3*	1.6	*1.5*	*0.8*	**1.0**	*0.5*	*1.0*	0.77
MAY	**1.0**	**–0.2**	0.6	0.7	**0.5**	1.4	**2.2**	**–0.1**	0.3	–0.1	0.66
JUN	0.6	*–0.3*	*0.1*	**–0.2**	0.3	**0.1**	0.1	0.0	0.6	**0.4**	0.66
JUL	**1.8**	1.1	0.7	1.2	0.8	**0.7**	**0.3**	**0.8**	*0.9*	**0.9**	0.65
AUG	0.8	**1.5**	0.5	0.9	1.2	**1.1**	**1.0**	0.8	**0.4**	0.9	0.68
SEP	0.5	1.1	**1.1**	*1.5*	0.7	**0.7**	0.4	1.0	**1.9**	0.5	0.67
OCT	0.4	0.9	–0.4	**0.9**	–0.8	0.3	0.2	0.3	*–0.4*	*0.3*	0.74
NOV	1.5	1.1	1.1	*2.5*	1.6	0.8	0.6	*1.0*	0.3	*1.7*	0.76
DEC	**2.8**	*0.9*	*0.2*	**2.8**	1.6	2.1	**2.6**	1.9	*0.7*	*1.7*	0.70

Table 2 Area average mean temperature change (°C) for Sweden between 1961–1990 and 1991–2020 for each cluster calculated from ERA5 data. Clusters for which the interquartile range of daily data changes by more than 0.5°C are marked with italics for decreased range and bold face for increased range. The rightmost column shows the corresponding northern hemisphere average warming according to HadCRUT5.

	1	2	3	4	5	6	7	8	9	10	TOTAL
JAN	**–14**	9	**7**	**5**	–14	**–27**	**–5**	14	*37*	*18*	8
FEB	–11	*–10*	*7*	*0*	–11	*–18*	–1	*16*	0	28	7
MAR	*8*	*–39*	–15	*19*	*–12*	*10*	*6*	**2**	*0*	–2	–7
APR	**–26**	**–13**	–11	**–7**	**–5**	**–4**	*–12*	–3	**27**	*7*	–6
MAY	*17*	*46*	*3*	*13*	*33*	25	1	11	25	17	15
JUN	–3	*46*	**29**	*38*	*35*	*28*	3	23	37	*16*	29
JUL	–32	1	**7**	10	0	**–12**	*5*	*24*	25	**–16**	5
AUG	18	17	*–3*	**11**	**–22**	7	4	*18*	*5*	*12*	5
SEP	–41	*8*	–51	**0**	4	7	–27	*–8*	*41*	**–11**	–10
OCT	**6**	*6*	–4	*–8*	**6**	–4	**61**	**14**	**–10**	**–47**	1
NOV	–3	–21	–12	–13	–7	–3	–12	**10**	–3	7	–4
DEC	*–2*	**–10**	**1**	19	12	–11	24	*13*	*3*	*–16*	1

Table 3 Area average mean change in precipitation intensity (%) for Sweden between 1961–1990 and 1991–2020 for each cluster and total for each month. Clusters for which the coefficient of variability (CV) of daily data changes by more than 10% are marked with italics for decreased range and bold face for increased range.

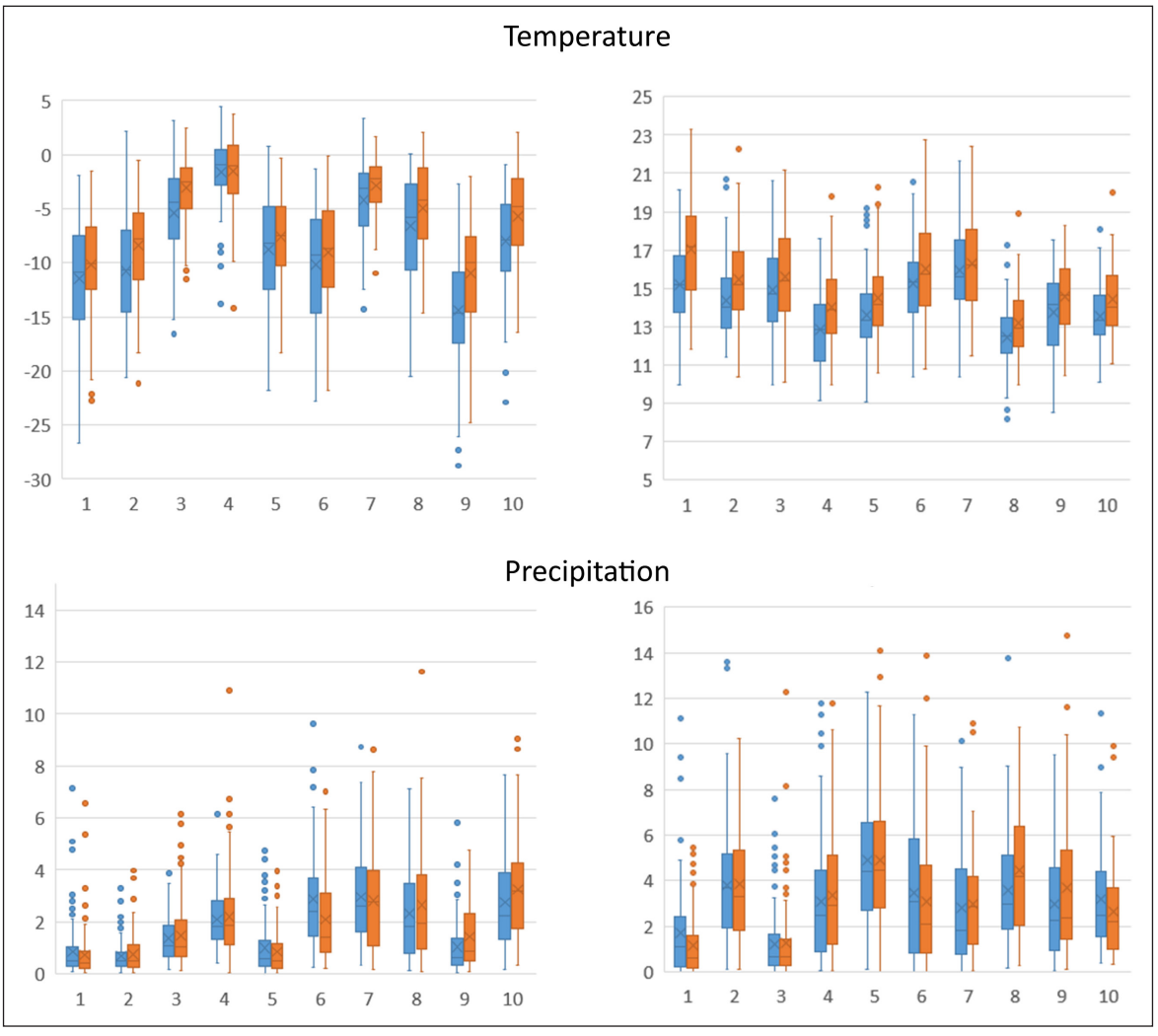

Figure 7 Distributions of daily data for the ten circulation types in January (left) and July (right). For each circulation type the blue boxplot represents 1961–1990 and the orange 1991–2020. The boxplots show the mean value represented with an x, the median represented by the central horizontal line, the 25th and 75th percentiles represented by the box. Points outside of 1.5 times the interquartile range from the respective 25th and 75th percentiles are considered to be outliers and are denoted by a point. The length of the whiskers is defined as the largest or smallest value not being an outlier. Units: °C for temperature and mm for precipitation.

range indicating larger variability in temperatures. The two CTs with smaller variability are CT4 and CT9, which both are associated with low pressure centres to the east of Scandinavia and winds from the northeast.

Generalizing to all months, the seasonal pattern is amplified. ***Table 2*** indicates that CTs with a decrease of the interquartile range exceeding 0.5°C are most common in November-March while an increase exceeding 0.5°C is most common in April-September. Naturally, changing the threshold to 0°C, to consider all CTs, changes the actual number of CTs showing increasing or decreasing variability. But the general pattern with reduced variability in winter and increased variability in summer does not change.

Also for precipitation there are CTs indicating increases and CTs indicating decreases in variability (***Table 3***). In contrast to temperature, however, the trends are less consistent between the seasons with tendencies for increase and decrease seen in both summer and winter.

Discrimination between changes in frequency and within-CT amplitude

Figures 8 and ***9*** show the monthly mean change between the two climate normals both as a total number and divided in its two components related to frequency and within-CT amplitude following Eq. 1. Both for temperature and precipitation it is clear that there are strong seasonal and geographical differences in the change signals.

For temperature, starting in November-December strong changes are seen in the northern parts of the domain, in particular in high-altitude areas (***Figure 8***). Subsequently, changes spread from these areas and from the far north to wider areas and in January a strong warming signal is seen over most of Scandinavia, still with pronounced maxima along the mountain chain. Continuing further into the winter and spring we note that changes are relatively smaller in an area in the interior parts of central and northern Scandinavia while larger changes are seen both in the mountains to the west, in the south and along the Baltic Sea coasts. Also in summer the strongest temperature changes are seen along the mountain chain. For June and October, with lower temperatures in the second climate normal in large parts of Sweden we note again strong positive change in the mountains but also over the Baltic Sea.

It is clear from the figure that the within-CT change dominates the temperature signal for most months

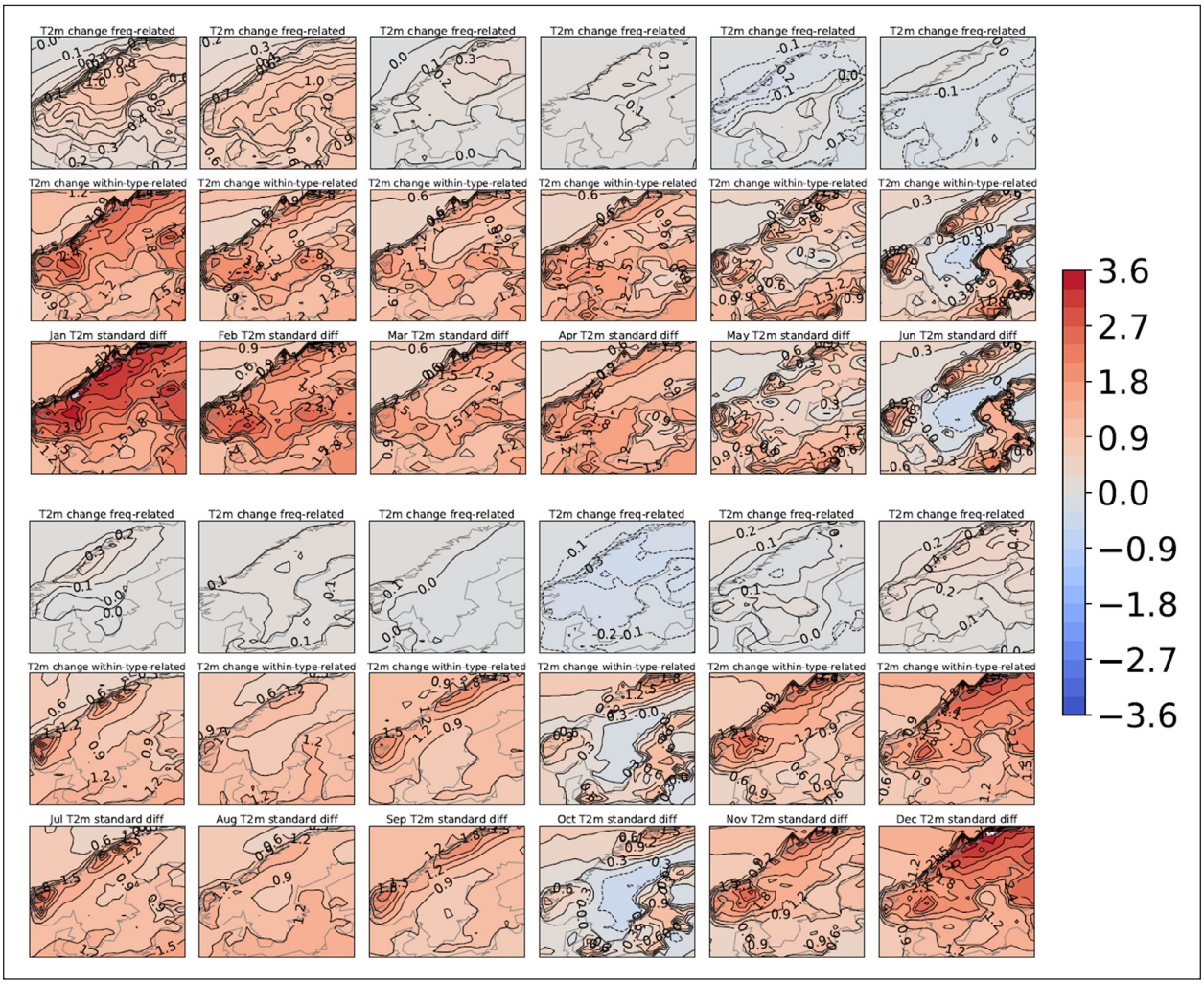

Figure 8 Temperature difference between 1961–1990 and 1991–2020 for January-June (upper part) and July-December (lower). The uppermost row for each month shows the difference that is due to changing frequencies of circulation types. The middle row shows the within-circulation type amplitude changes. The lowermost row shows the total changes. Units: °C.

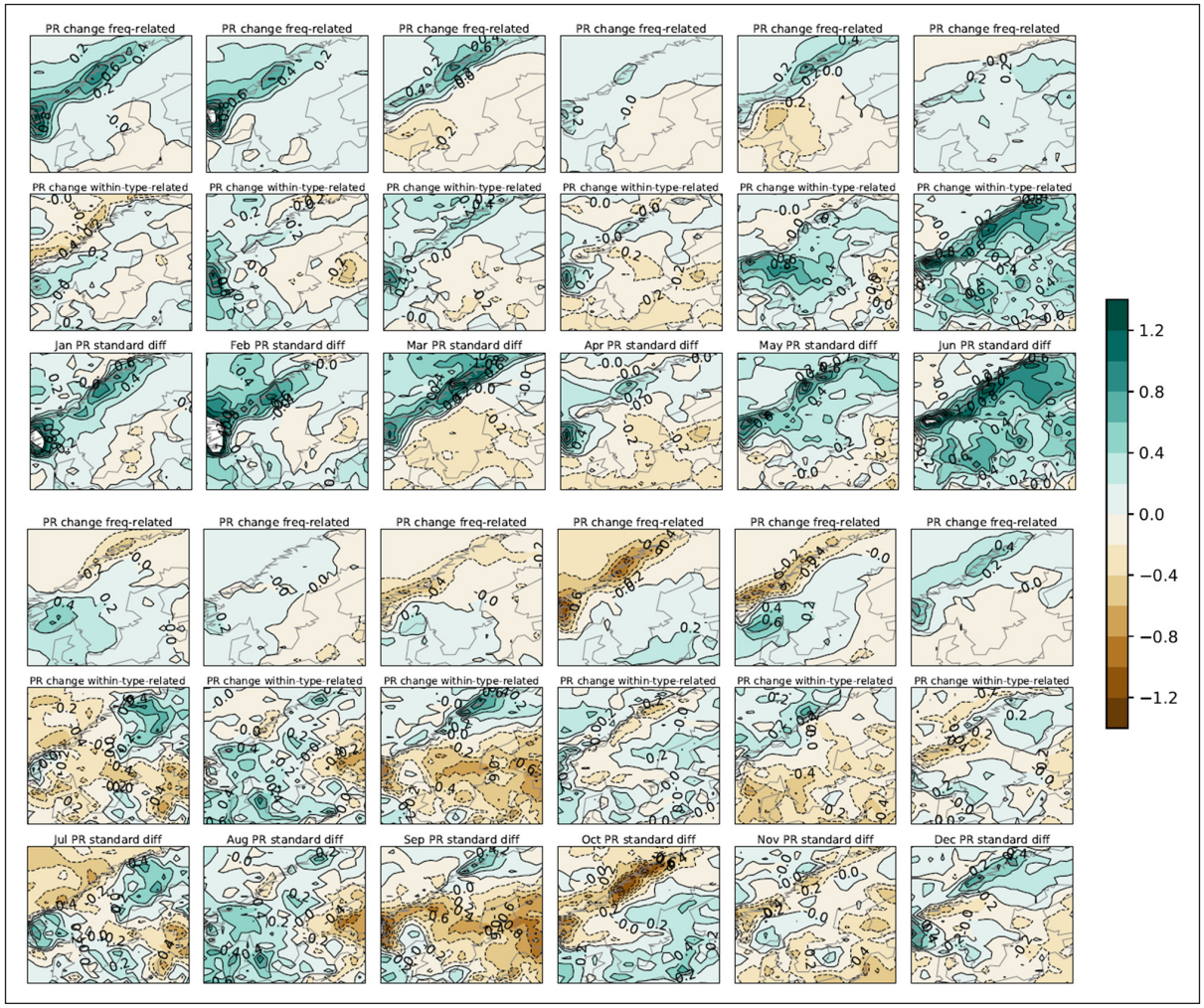

Figure 9 As Figure 8, except for precipitation. Units: mm/day.

in all of the domain. Both the geographical patterns and the amplitude of the within-CT changes are very similar to the total signal. There are, however, some notable contributions from frequency-related changes. The largest ones are seen as strong contributions to the warming in January and February. In February, the contribution even exceeds the contribution from within-CT change for parts of Northern Sweden. Also for other months, there are frequency-related contributions to warming like in March, July and December or cooling as in May, June and October. In general, frequency-related changes are more geographically homogeneous than the within-CT changes that appear to be more influenced by orography, extension of snow cover and land-sea contrasts.

For precipitation (***Figure 9***) the differences are less coherent than those found for temperature. The figures show a mixed pattern with months showing either increasing or decreasing precipitation in different parts of the domain. A general increase in precipitation in the first six months of the year is seen for large parts of Norway and the mountain chain while changes to the east, in Sweden, have different signs. The strongest area increase is found for June while September shows the largest decrease.

As a stark contrast to temperature, the frequency-related contributions for precipitation are relatively larger. In some areas and months, it is even dominating the signal like in the mountain chain in January and February. In other areas and months, the two counteract each other like in south-eastern Norway and southern Sweden in May that would have seen a decrease in precipitation if it only were for frequency-related changes. In reality, the within-CT strong increase even leads to overall increasing precipitation in the area. For other months, the within-CT changes dominate the picture, like in April and June. Also for precipitation we note that the frequency-related fields are smoother than the within-CT changes, indicating a more geographically homogeneous response. However, in contrast to temperature, there are stronger regional features associated with orography, evidently most pronounced along the mountain chain but also, to some extent, visible over southern Sweden where extensive areas are more than 200 m above sea level.

DISCUSSION

POTENTIAL MECHANISMS BEHIND THE CHANGES IN TEMPERATURE AND PRECIPITATION

Global warming, resulting primarily from increasing greenhouse gas content, shows strong geographical differences (IPCC, 2021). Such differences in warming lead to changes in zonal and meridional temperature gradients that, in turn, may have an impact on the large-scale atmospheric circulation. The strong warming in the Arctic and its potential impact on lower latitudes have received strong attention over the last years but it is still uncertain to what degree there is an impact on mid-latitude circulation (Doblas-Reyes et al., 2021). The uncertainty is to a strong degree associated with the relatively short observational time series and the large natural internal variability in the climate.

Related to the analysed CT changes we discriminate between changes in frequency of different CTs, exemplified by the decreases in frequency of CT9 in January and CT3 in July (***Figure 4***), and changes within CTs, such as the changes in pressure gradients associated with CT4 and CT9 in January (***Figure 5***). The distinction between frequency-related changes and within-circulation type changes shows, similar to what was found by Kuettel et al (2011), that within-type changes dominate for temperature. For precipitation, however, we note that frequency-related changes have a relatively large impact (***Figure 9***). Compared to Kuettel et al. we use higher-resolution data and note that this may explain some differences as it better resolves dynamical features related to orography, which appears to be strongly linked to the higher degree of frequency-related differences for precipitation than for temperature.

In addition to frequency-related changes and within-circulation type changes, changes in local climate conditions can also result from airmasses being advected from regions that have seen more or less warming and/or moistening and from local changes in forcing conditions and feedback processes. Which of these mechanisms are responsible for the observed changes and to what degree cannot be determined in detail from the simple analysis of CTs performed here. For Europe, however, we note that the observed warming over the last decades is strongest over the northern, central and eastern parts, while western areas and the adjacent North Atlantic have seen less warming (Gulev et al., 2021). This indicates that airmasses being advected towards Scandinavia have changed differently for different directions. We reiterate here that the westerly circulation type CT4 in January shows only small changes in temperature over Scandinavia (***Figure 5***), likely a result of relatively modest changes in sea surface temperatures over the North Atlantic. At the same time the cold circulation type CT9, associated with easterly winds shows very strong warming over much of the region, which may be related to warmer conditions in general over eastern Europe and Russia. We also note that the strong within-type changes seen for temperature in mountainous regions indicate that local feedback processes related to changes in snow conditions have a strong impact on the observed changes during all seasons in this region (***Figure 8***). Similarly, feedback processes in the Baltic Sea appear to have an impact for some specific months. To analyse such differences more in-depth we suggest to explore the combination of CT classification and climate model simulations with different imposed changes in regional forcing conditions.

RELATION TO VARIATIONS IN THE NAO-INDEX

The NAO-index is often used to relate changes in climatological variables in Northern Europe to changes in large-scale atmospheric circulation (e.g. Hegerl et al., 2018). For Sweden, we present results from a regression analysis between the NAO-index and respectively temperature and precipitation for the two periods in ***Table 4***. We note that there is partly a strong positive

NORMAL PERIOD	SEASON	NAO	R^2		K		L	
			T	PR	T	PR	T	PR
1961–1990	DJF	–0.25	0.59	0.17	1.70	11.7	–4.22	136
	MAM	0.02	0.38	0.04	1.17	10.5	3.18	114
	JJA	0.13	0.09	0.02	0.74	–17.6	14.5	205
	SON	0.07	0.35	0.00	1.00	0.23	5.51	193
1991–2020	DJF	0.37	0.61	0.24	1.38	14.9	–3.31	143
	MAM	0.13	0.46	0.02	0.99	4.92	4.29	119
	JJA	–0.08	0.03	0.21	0.42	–42.9	15.5	226
	SON	–0.10	0.28	0.02	1.39	10.9	6.39	189

Table 4 30-year average NAO-index and results from linear fits with temperature (T) and precipitation (PR) from the Swedish average derived from the SMHI stations. The linear fits are done separately over the two 30-year periods. The regression coefficients (r^2), slopes (k) and intercepts (l) are given.

correlation between the NAO-index and temperature. For instance, we note that more than 55% of the interannual variability can be explained by the NAO-index in winter. In summer, correlation is much smaller (<10%) and in spring and fall it lies in between. Also for precipitation some correlation can be expected as seen from the distinct patterns in precipitation in ***Figure 3***. However, when averaged over all of Sweden, positive and negative contributions partly cancel out and the correlation is relatively low for all seasons. Again, the highest numbers are found in winter with a correlation explaining about 20% of the variability.

Comparing the two periods, it is clear that there are differences in the NAO-index. For winter there is a shift from a negative number in the first climate normal to a positive number in the second. This is a result of similar changes in all three winter months, mostly pronounced in February (not shown). Also in spring, the second period is on average more NAO positive due to increases in March and April, while in summer and fall the second period is more NAO negative. The strongest tendencies towards more NAO negative numbers are found for June and October. We also note that the intercept (*I*) increases for temperature for all seasons indicative of the warmer climate. The correlation is similar in both periods for temperature apart from fall where it drops from 0.35 to 0.22, which could potentially indicate that conditions in fall change from being more "winter-like" to more "summer-like" in the second period. Also for precipitation the degree of correlation between the two periods is similar with the exception for summer where it increases from 0.02 to 0.22 in the second period indicating a stronger anticorrelation with on average less precipitation the warmer it is.

TEMPERATURE AND PRECIPITATION CHANGES DERIVED FROM ANALYSIS OF CHANGES IN THE LARGE-SCALE CIRCULATION

As summarized in ***Figures 8*** and ***9***, results obtained from the CTC and the decomposition following Barry and Perry (1973) clearly show that part of the changes between 1961–1990 and 1991–2020 are related to changes in large-scale circulation. In detail this is related to changes in individual CTs such as, for instance, the strong reduction in frequency for the cold CT9 in January (***Figures 2*** and ***4***) which contributes to the warming between the two periods. We note, however, that changes within CT9 are also very large (***Figure 5***). Similarly, changes in the frequency of CT3 and CT6 in July as shown in ***Figure 4*** are expected to impact differences in temperature and precipitation in different parts of the country (***Figures 3*** and ***6***). Results for both temperature and precipitation indicate that the fraction of explained change, due to frequency-related changes and/or within-CT related changes, differs between different months and in different locations (***Figures 8*** and ***9***). The analysis of changes in the NAO-index corroborates the picture as it also indicates milder conditions during winter in the latter period, resulting from more NAO-positive conditions on average.

The results, both for changes in CTs and in NAO-index, also show that changes in large-scale conditions can only explain parts of the differences between the two periods and that there are strong changes also within each CT. Here, we summarize this by setting up two simple models for the temperature and precipitation climate in 1991–2020 based on the relation between these variables and the large-scale circulation as given by the CT analysis and by the NAO-index. For our "NAO model" we use the result from linear regressions of temperature and precipitation against the NAO-index for all twelve calendar months based on the full 1961–2020 time period. The regression coefficients are then used with the NAO-index to derive synthetic temperature and precipitation values for all individual months in 1961–2020. Subsequently, we calculate differences between the two periods based on these synthetic numbers. In a similar way we set up a "CT-based model" by taking the average temperature and precipitation for 1961–1990 for each CT and then multiplying by the frequency of the CTs in the 1991–2020 period. We compare the change in climate between both these synthetic "models" for 1991–2020 average Swedish conditions with the actual observed difference in ***Figure 10***. As already indicated

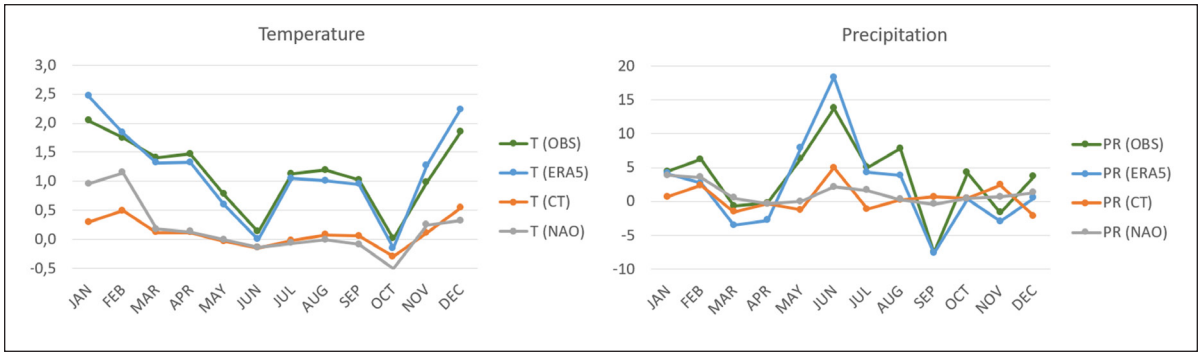

Figure 10 Changes in Swedish mean temperature (left, °C) and precipitation (right, mm/month) between 1961–1990 and 1991–2020. Observations (green) are from the SMHI data, reanalysis (blue) from ERA5. The synthetic temperature and precipitation series are derived from changes in the NAO-index (grey) and the analysis of circulation types (orange). See text.

above, it is clear that the large-scale circulation related changes can only explain a fraction of the change in Swedish average temperature and precipitation. For temperature, the degree of explanation is largest for the winter months (cf. ***Figure 8***). We also note that the relatively cold conditions in June and October can partly be explained by large-scale circulation changes. For precipitation, circulation-based changes in January and February contribute to explain the observed differences. For other months, the degree of explained changes is small. Notably, there is a contribution to the increased precipitation in June from the large-scale circulation as also seen in ***Figure 9***.

METHODOLOGICAL ISSUES

The results show distinct differences in both temperature and precipitation for the different CTs. A potential effect that could influence our interpretation would be systematic changes in timing of CTs. In particular, during spring and fall when temperature differences between early and late parts of a month are large shifts in timing could influence the results. A systematic difference of three days (10% of a month) could result in an artificial temperature difference by a few tenths of a degree in a month with large temperature trends. To check if this is the case we have calculated the average date number for each CT and each month in the two periods. Differences of up to several days are noted for individual CTs and months but in general differences are within plus minus two days and it is only in four out of the 120 combinations (10 CTs x 12 months) that they exceed four days (not shown). We conclude that systematic differences in timing are not important for the interpretation of our results.

Another potential source of error emanates from the "blurring" of results as we look at daily averages. In reality, the CTs shift in a more continuous way with different weather situations sometimes occurring on the same day. As it is now we assign the full day to a certain CT implying that we are occasionally blending results from both cold and warm air mass weather on the same day. This blending is likely a contributing cause to the relatively large variability within some CTs (cf. ***Figure 7***). We have not made any attempts to quantify this potential error or compensate for it and it could be suggested as a possible extension to this work. At the same time, however, we note that any potential impact from it would be similar in the two periods so it is unlikely that any of the conclusions would change.

CONCLUSIONS

We present a detailed analysis of change in temperature and precipitation in northern Europe between the two climate normals 1961–1990 and 1991–2020. Results indicate that all seasons have become warmer and that the warming is generally larger than the hemispheric mean. The results also show a clear decrease in daily temperature variability for winter and an increase in summer. For precipitation observations indicate an increase in the Swedish average in eight out of twelve months, changes close to zero for three, and only in one month, September, there is a decrease. The reanalysis also shows an increase, albeit smaller, both expressed in absolute and relative numbers. We speculate that this difference may either reflect errors related to sampling in the station data, or deficiencies in the forecast model used to produce ERA5, or representativity issues when comparing spatial fields from the reanalysis to an estimate based on c. 70 stations. There is no clear indication of a systematic change in daily precipitation variability.

In a subsequent step the analysis is conditioned on large-scale circulation patterns as given by the SANDRA circulation type classification method. The different circulation types (CTs) generated individually for each month resemble each other, in particular within the winter period and within the summer period. As expected, it is shown that they are associated with strong anomalies in temperature and precipitation with distinct regional features. Not only averages and spatial patterns differ between CTs but also daily variability in both temperature and precipitation.

The analysis of the CTs shows that changes between the two periods can partly be related to changes in large-scale circulation due to changes in the frequencies of different CTs. However, it is also clear that the contribution from frequency-related changes to the total temperature change is comparatively low for most months and that changes also within each CT are required to explain the total change. For temperature, the largest contribution from frequency-related changes are seen in January and February when about half of the increase in temperatures can be attributed to generally more zonal conditions. The results also indicate that changes in daily variability are strongly dependent on circulation type. It is illustrated that the largest reduction in temperature variability seen in winter is related to decreased variability in cold high-pressure type situations while the low-pressure dominated periods with strong advection of mild air from the Atlantic do not see large changes. For summer, contrastingly, temperature variability increases for all weather types.

For precipitation, the contribution of frequency-related changes to the overall changes are sometimes larger than for temperature. This is particularly seen in areas close to high-altitude areas like the Scandes mountain chain as a result of orographic reinforcement. Such reinforcement is also noted for other parts of Scandinavia like southern Sweden where the highland area, despite moderate height of a few hundred meters, influences precipitation in different directions of the large-scale flow. Averaged

over all of Sweden the precipitation changes are to some extent cancelling out which makes it difficult to explain the change signal between the periods by use of the CTs alone. This may also be the reason for why we do not find any systematic changes in variability as for temperature. We note, however, that by investigating in more detail changes in mean sea level pressure distributions within the CTs we can identify potential explanations for the observed changes. For example, we find a number of areas where altered pressure gradients for some CTs contribute to regional changes in precipitation in both summer and winter.

A comparison with a simple analysis of the NAO-index reveals many similarities, such as the larger contribution from changes in CTs to changes in temperature and precipitation during winter. But, also, it is clear that the CT analysis reveals more details and can give a more comprehensive picture of climate and changes between periods. Simple empirical models that were set up to model temperature and precipitation characteristics of 1991–2020 based on circulation changes combined with relations from the 1961–1990 climate normal failed to explain the full warming and gave only very little information about precipitation changes between the periods. This summarizes in a clear way that changes between the two periods are only partly determined by changes in CTs. We conclude, that internal climate variability, as represented by changes in large-scale atmospheric circulation, cannot explain the observed changes in temperature and precipitation in Sweden. A main conclusion of the study is that during the last 30 years it has mostly been warmer than in the preceding 30 years for the same type of weather situation for all months in the year.

ACKNOWLEDGEMENTS

EU COST Action 733 is acknowledged for producing and making available the clustering software. We acknowledge the ECMWF for providing the ERA5 data, the CRU for providing the HadCRUT5 data and NCAR for providing the NAO index.

COMPETING INTERESTS

The authors have no competing interests to declare.

AUTHOR AFFILIATIONS

Erik Kjellström *orcid.org/0000-0002-6495-1038*
Rossby Centre, Swedish Meteorological and Hydrological Institute, SMHI, Norrköping, SE-602 19, SE; Department of Meteorology and Bolin Centre for climate research, Stockholm University, Stockholm, SE-106 91, SE

Felicitas Hansen *orcid.org/0000-0003-4696-3059*
Rossby Centre, Swedish Meteorological and Hydrological Institute, SMHI, Norrköping, SE-602 19, SE; Institute of Coastal Systems, Helmholtz-Zentrum Hereon, Geesthacht, DE-21502, DE

Danijel Belušić *orcid.org/0000-0002-5665-3866*
Rossby Centre, Swedish Meteorological and Hydrological Institute, SMHI, Norrköping, SE-602 19, SE; Department of Geophysics, Faculty of Science, University of Zagreb, 10000 Zagreb, HR

REFERENCES

Barry, RG and **Perry, AH.** 1973. *Synoptic Climatology: methods and applications*. London: Methuen.

Beck, C, Jacobeit, J and **Jones, PD.** 2007. Frequency and within-type variations of large-scale circulation types and their effects on low-frequency climate variability in Central Europe since 1780. *Int. J. Climatol*., 27(4): 473–491. DOI: *https://doi.org/10.1002/joc.1410*

Bhend, J and **von Storch, H.** 2009. Is greenhouse gas forcing a plausible explanation for the observed warming in the Baltic Sea catchment area? *Boreal Environ. Res*, 14: 81–88.

Busuioc, A, Chen, D and **Hellström, C.** 2001. Temporal and spatial variability of precipitation in Sweden and its link with the largescale atmospheric circulation. *Tellus A: Dyn. Meteorol. Oceanogr,* 53: 348–367. DOI: *https://doi.org/10.1034/j.1600-0870.2001.01152.x*

Cahynova, M and **Huth, R.** 2016. Atmospheric circulation influence on climatic trends in Europe: an analysis of circulation type classifications from the COST733 catalogue. *Int. J. Climatol*, 36(7, SI): 2743–2760. DOI: *https://doi.org/10.1002/joc.4003*

Cattiaux, J, Vautard, R, Cassou, C, Yiou, P, Masson-Delmotte, V and **co-authors.** 2010. Winter 2010 in Europe: A cold extreme in a warming climate. *Geophys. Res. Lett*, 37: L20704. DOI: *https://doi.org/10.1029/2010GL044613*

Doblas-Reyes, FJ, Sörensson, AA, Almazroui, M, Dosio, A, Gutowski, WJ, Haarsma, R, Hamdi, R, Hewitson, B, Kwon, W-T, Lamptey, BL, Maraun, D, Stephenson, TS, Takayabu, I, Terray, L, Turner, A and **Zuo, Z.** 2021. Linking Global to Regional Climate Change. In: *Climate Change 2021: The Physical Science Basis. Contribution of Working Group I to the Sixth Assessment Report of the Intergovernmental Panel on Climate Change*, Masson-Delmotte, V, Zhai, P, Pirani, A, Connors, SL, Péan, C, Berger, S, Caud, N, Chen, Y, Goldfarb, L, Gomis, MI, Huang, M, Leitzell, K, Lonnoy, E, Matthews, JBR, Maycock, TK, Waterfield, T, Yelekçi, O, Yu, R and Zhou, B (eds.). Cambridge University Press. In Press.

Gulev, SK, Thorne, PW, Ahn, J, Dentener, FJ, Domingues, CM, Gerland, S, Gong, D, Kaufman, DS, Nnamchi, HC, Quaas, J, Rivera, JA, Sathyendranath, S, Smith, SL, Trewin, B, von Shuckmann, K and **Vose, RS.** 2021. Changing State of the Climate System. In: *Climate Change 2021: The Physical Science Basis. Contribution of Working Group I to the Sixth Assessment Report of the Intergovernmental Panel on*

Climate Change, Masson-Delmotte, V, Zhai, P, Pirani, A, Connors, SL, Péan, C, Berger, S, Caud, N, Chen, Y, Goldfarb, L, Gomis, MI, Huang, M, Leitzell, K, Lonnoy, E, Matthews, JBR, Maycock, TK, Waterfield, T, Yelekçi, O, Yu, R and Zhou, B (eds.). Cambridge University Press. In Press.

Hansen, F and **Belušić, D.** 2021. Tailoring circulation type classification outcomes. *Int. J. Climatol*., 41(14): 6145–6161. DOI: *https://doi.org/10.1002/joc.7171*

Hawkins, E and **Sutton, R.** 2009. The potential to narrow uncertainty in regional climate predictions. *Bull. Am. Meteorol. Soc*, 90: 1095–1107. DOI: *https://doi.org/10.1175/2009BAMS2607.1*

Hawkins, E and **Sutton, R.** 2012. Time of emergence of climate signals. *Geophys. Res. Lett*. 39: L01702. DOI: *https://doi.org/10.1029/2011 GL050087*

Hegerl, G and **Zwiers, F.** 2011. Use of models in detection and attribution of climate change. *WIREs Clim. Change,* 2(4), 570– 591. DOI: *10.1002/wcc.121*

Hegerl, GC, Brönnimann, S, Schurer, A and **Cowan, T.** 2018. The early 20th century warming: Anomalies, causes, and consequences. *WIREs Clim. Change*, 9: e522. DOI: *https://doi.org/10.1002/wcc.522*

Hersbach, H, Bell, B, Berrisford, P, Hirhara, S, Horányi, A and **co-authors.** 2020. The ERA5 global reanalysis. *Q. J. R. Meteorolog. Soc*. 146: 1999– 2049. DOI: *https://doi.org/10.1002/qj.3803*

Hurrell, JW. 1995. Decadal trends in the North Atlantic oscillation: regional temperatures and precipitation. *Science,* 269: 676–679.

IPCC. 2018. Global warming of 1.5°C. *An IPCC Special Report on the impacts of global warming of 1.5°C above pre-industrial levels and related global greenhouse gas emission pathways, in the context of strengthening the global response to the threat of climate change, sustainable development, and efforts to eradicate poverty*. Cambridge & New York: Cambridge University Press.

IPCC. 2019. *IPCC Special Report on the Ocean and Cryosphere in a Changing Climate*, Pörtner, H-O, Roberts, DC, Masson-Delmotte, V, Zhai, P, Tignor, M, Poloczanska, E, Mintenbeck, K, Alegría, A, Nicolai, M, Okem, A, Petzold, J, Rama, B and Weyer, NM (eds.). In press.

IPCC. 2021. Summary for Policymakers. In: *Climate Change 2021: The Physical Science Basis. Contribution of Working Group I to the Sixth Assessment Report of the Intergovernmental Panel on Climate Change*, Masson-Delmotte, V, Zhai, P, Pirani, A, Connors, SL, Péan, C, Berger, S, Caud, N, Chen, Y, Goldfarb, L, Gomis, MI, Huang, M, Leitzell, K, Lonnoy, E, Matthews, JBR, Maycock, TK, Waterfield, T, Yelekçi, O, Yu, R and Zhou, B (eds.). Cambridge University Press. In Press.

Kjellström, E. 2004. Recent and future signatures of climate change in Europe. *Ambio*, 33(4–5): 193–198.

Kjellström, E, Nikulin, G, Hansson, U, Strandberg, G and **Ullerstig, A.** 2011. 21st century changes in the European climate: uncertainties derived from an ensemble of regional climate model simulations. *Tellus A: Dyn. Meteorol. Oceanogr,* 63(1): 24–40. DOI: *https://doi.org/10.1111/j.1600-0870.2010.00475.x*

Kjellström, E, Thejll, P, Rummukainen, M, Christensen, JH, Boberg, F and **co-authors.** 2013. Emerging regional climate change signals for Europe under varying large-scale circulation conditions. *Clim. Res.*, 56: 103–119. DOI: *https://doi.org/10.3354/cr01146*

Kuettel, M, Luterbacher, J and **Wanner, H.** 2011. Multidecadal changes in winter circulation-climate relationship in Europe: frequency variations, within-type modifications, and long-term trends. *Clim. Dyn*., 36(5–6): 957–972. DOI: *https://doi.org/10.1007 /s00382-009-0737-y*

Morice, CP, Kennedy, JJ, Rayner, NA, Winn, JP, Hogan, E and **co-authors.** 2021. An updated assessment of near-surface temperature change from 1850: the HadCRUT5 dataset. *J. Geophys. Res. D: Atmos.,* 126: e2019JD032361. DOI: *https://doi.org/10.1029/2019JD032361*

NCAR. 2021. National Center for Atmospheric Research Staff (Eds). Last modified 05 Jun 2021. "The Climate Data Guide: Hurrell North Atlantic Oscillation (NAO) Index (PC-based)." Retrieved from *https://climatedataguide.ucar.edu/climate-data/hurrell-north-atlantic-oscillation-nao-index-pc-based*.

Parding, KM, Liepert, BG, Hinkelman, LM, Ackerman, TP, Dagestad, K-F and **co-authors.** 2016. Influence of synoptic weather patterns on solar irradiance variability in northern Europe. *J. Clim.,* 29(11): 4229– 4250. DOI: *https://doi.org/10.1175/JCLI-D-15-0476.1*

Philipp, A, Della-Marta, PM, Jacobeit, J, Fereday, DR, Jones, PD and **co-authors.** 2007. Long-term variability of daily North Atlantic-European pressure patterns since 1850 classified by simulated annealing clustering. *J. Clim.,* 20(16): 4065–4095. DOI: *https://doi.org/10.1175/JCLI 4175.1*

Philipp, A, Bartholy, J, Beck, C, Erpicum, M, Esteban, P and **co-authors.** 2010. Cost733cat-A database of weather and circulation type classifications. *Phys. Chem. Earth.,* 35(9–12): 360–373. DOI: *https://doi.org/10.1016/j.pce.2009.12.010*

Philipp, A, Beck, C, Huth, R and **Jacobeit, J.** 2016. Development and comparison of circulation type classifications using the COST 733 dataset and software. *Int. J. Climatol*., 36: 2673–2691. DOI: *https://doi.org/10.1002/joc.3920*

Rutgersson, A, Jaagus, J, Schenk, F and **Stendel, M.** 2014. Observed changes and variability of atmospheric parameters in the Baltic Sea region during the last 200 years. *Clim. Res.,* 61: 177–190. DOI: *https://doi.org/10.3354/cr01244*

Sui, C, Yu, L and **Vihma, T.** 2020. Occurrence and drivers of wintertime temperature extremes in Northern Europe during 1979–2016. *Tellus A: Dyn. Meteorol. Oceanogr,* 72(1): 1–19. DOI: *https://doi.org/10.1080/16000870.2020.1788368*

Van Ulden, AP and **van Oldenborgh, GJ.** 2006. Large-scale atmospheric circulation biases and changes in global climate model simulations and their importance for climate change in Central Europe. *Atmos. Chem. Phys*, 6: 863–881.

Wilcke, R Kjellström, E, Liu, C, Matei, K and **Moberg, A.** 2020. The extreme warm summer 2018 in Sweden – set in a historical context. *Earth Syst. Dyn,* 11: 1107–1121. DOI: *https://doi.org/10.5194/esd-11-1107-2020*

TO CITE THIS ARTICLE:
Kjellström, E., & Hansen, F., & Belušić, D. 2022. Contributions from Changing Large-Scale Atmospheric Conditions to Changes in Scandinavian Temperature and Precipitation Between Two Climate Normals. *Tellus A: Dynamic Meteorology and Oceanography*, 74(2022), 204–221. DOI: *https://doi.org/10.16993/tellusa.49*

Submitted: 23 March 2022 Accepted: 23 March 2022 Published: 18 April 2022